

Magnetization current simulation of high temperature bulk superconductors using A-V-A formula based iterative algorithm method

Kai Zhang, Sebastian Hellmann, Marco Calvi ^{*}, Thomas Schmidt

Paul Scherrer Institute, Villigen, CH, 5232

Lucas Brouwer

Lawrence Berkeley National Laboratory, Berkeley, CA, 94720

^{} To whom correspondence should be addressed: marco.calvi@psi.ch*

Abstract

In this work we will introduce the **A-V-A** formula based iterative algorithm method (IAM) for simulating the magnetization of superconductors. This new method is for the first time tested in simulating both the critical state model and the flux creep model based magnetization process in a disk-shaped ReBCO bulk. The computation time is saved by using **A-V** formula in superconductor area and **A**-formula in non-superconductor area. We confirm it is feasible to simulate the trapped current density in the ReBCO bulk during zero field cooling (ZFC) or field cooling (FC) magnetization after comparing the simulation results from using COMSOL **H**-formula. Specially, IAM is proved friendly to add ferromagnetic materials into the FEA model and to take into account the magnetic field-dependent or mechanical strain-related critical current density of the superconductor. The influence factors for magnetization simulation, like the specified iterative load steps, the initial resistivity and the ramping time, are discussed in detail. The **A-V-A** formula based IAM, implemented in ANSYS, shows its unique advantages in adjustable computation time, multi-frame restart analysis, easy-convergence and etc.

Keywords

A-V-A formula, ANSYS, iterative algorithm method, magnetization current, field cooling magnetization

1. Introduction

Magnetization current (screening current, shielding current or persistent current) effect of commercial superconductors, usually un-desired, has been extensively studied in superconducting accelerator magnets [1-7], NMR magnets and high T_c superconducting coils [8-17] by using numerical simulation or experimental method. Recent studies

show growing interests of using commercial FEM software, in which E - J power law based equations can be defined, to solve AC/DC magnetization problems for high T_c superconductors. Generally the form of Maxwell's equations defined for eddy current solver in the FEM software can be **A-V** [18-22], **T- Ω** [23-26], **T-A** [27-29] or **H**-formula [30-35].

The magnetization effects can also be beneficial

when we would like to trap magnetic field into high T_c superconducting bulks or tape stacks [36-43]. The common techniques for magnetizing the bulk or tape stack include zero field cooling (ZFC), field cooling (FC) and pulsed field magnetization (PFM). To simulate the magnetization process the available FEM software which can solve the critical state model [44] or the flux creep model [45-46] can be FLUX2D/3D [20, 23], COMSOL [31, 33, 47], FlexPDE [48-49], GetDP [19], Photo-eddy [21-22] or ANSYS [50-51]. Among these FEM tools COMSOL shows its special advantages in coupling user-defined partial differential equations, choosing the form of Maxwell's equations and conducting multi-physics coupled simulations [41, 52]. The other widely used multi-physics software ANSYS, available for secondary development by using ANSYS Parametric Design Language (APDL), has also been explored by scientists to solve AC magnetization problems of high T_c superconductors based on the proposed Resistivity-Adaption-Algorithm [50-51, 53]. This algorithm aims at finding a final resistivity matrix for the meshed superconductor elements to fulfill the critical state model or the E - J power law based flux creep model. But the intermediate magnetization process and the relaxation of magnetization are missed.

This paper, for the first time, explores the magnetization process of high T_c bulk superconductors during ZFC and FC magnetization by using the newly developed A - V - A formula based iterative algorithm method (IAM). The IAM, implemented in ANSYS APDL, proves feasible to

simulate the magnetization current of bulk superconductors in both the critical state model and the flux creep model. Specially, A - V formula is used in superconductor area to calculate both the magnetic field and the eddy current while A -formula is used in non-superconductor area to calculate only the magnetic field. Hence we name this method A - V - A formula.

The pre-installed A - V formula for eddy current solver is as follows

$$\nabla \times \left(\frac{1}{\mu} \nabla \times \mathbf{A} \right) = -\frac{1}{\rho} \left(\frac{\partial \mathbf{A}}{\partial t} + \nabla \cdot \mathbf{V} \right) \quad (1)$$

The current density \mathbf{J} equals to the right side of (1). For the critical state model the resistivity can be expressed as

$$\rho = \begin{cases} 0 & \text{if } |\mathbf{J}| \leq J_c(B) \\ +\infty & \text{if } |\mathbf{J}| > J_c(B) \end{cases} \quad (2)$$

where $J_c(B)$ refers to the magnetic field-dependent critical current density. For E - J power law based flux creep model the resistivity can be expressed as

$$\rho = \frac{E_c}{J_c(B)} \cdot \left(\frac{|\mathbf{J}|}{J_c(B)} \right)^{n-1} \quad (3)$$

where E_c refers to the transitional electrical field (usually 10^{-4} V/m).

The computation time of using ANSYS-IAM to solve magnetization current is competitive with COMSOL or other FEM tools. Other advantages of using this new method to solve magnetization problems are introduced in this paper.

2. The critical state model based iterative algorithm and its application in ZFC and FC magnetization

2.1. ZFC magnetization - external field rises from zero to 1 T

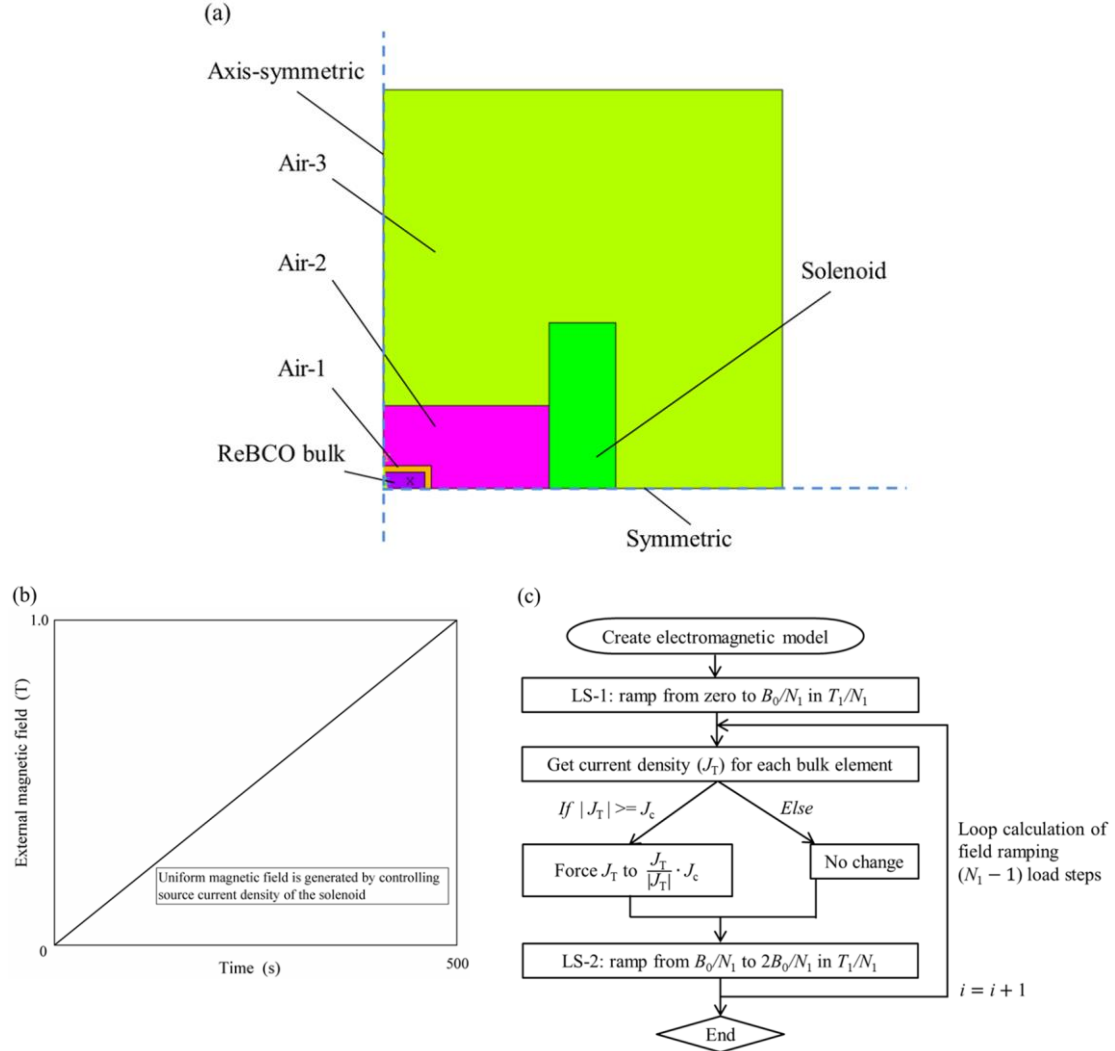


Figure 1. (a) 2D axis-symmetric half FEA model for magnetization current simulation of the ReBCO bulk (the solenoid is used to generate uniform magnetic field); (b) ZFC magnetization - external magnetic field going through the ReBCO bulk rises linearly from zero to 1 T in 500 seconds; (c) Iterative algorithm method for simulating the critical state model based ZFC magnetization ($J_c=3 \times 10^8$ A/m², $B_0=1$ T, $T_1=500$ s, $N_1=200$). This FEA model partially refers to the benchmark [54] given by COMSOL.

Figure 1 (a) shows the 2D axis-symmetric half FEA model created in ANSYS to simulate magnetization current in a disk-shaped ReBCO bulk ($\Phi 25$ mm, 10 mm thick) [54]. To approach the superconducting state, an initial resistivity ρ_0 of 10^{-16} $\Omega \cdot \text{m}$ is assigned to the ReBCO bulk for transient electromagnetic analysis.

Furthermore, to save the computation time, we consider eddy current is only generated in the ReBCO bulk by not assigning a resistivity to the air or the

solenoid. In the electromagnetic model the 8-nodes 2D element-type of *Plane233* is defined. *Plane233* having the freedom degree of *A* is named ET-1 and *Plane233* having the freedom degree of *A* and *V* is named ET-2. Initially the ReBCO bulk is meshed with ET-2 (*Plane233, A-V*) while non-superconductor areas are meshed with ET-1 (*Plane233, A*). After meshing the whole FEA model we apply symmetric boundary (flux normal) to the bottom line and apply flux parallel boundary to the two outer lines. The

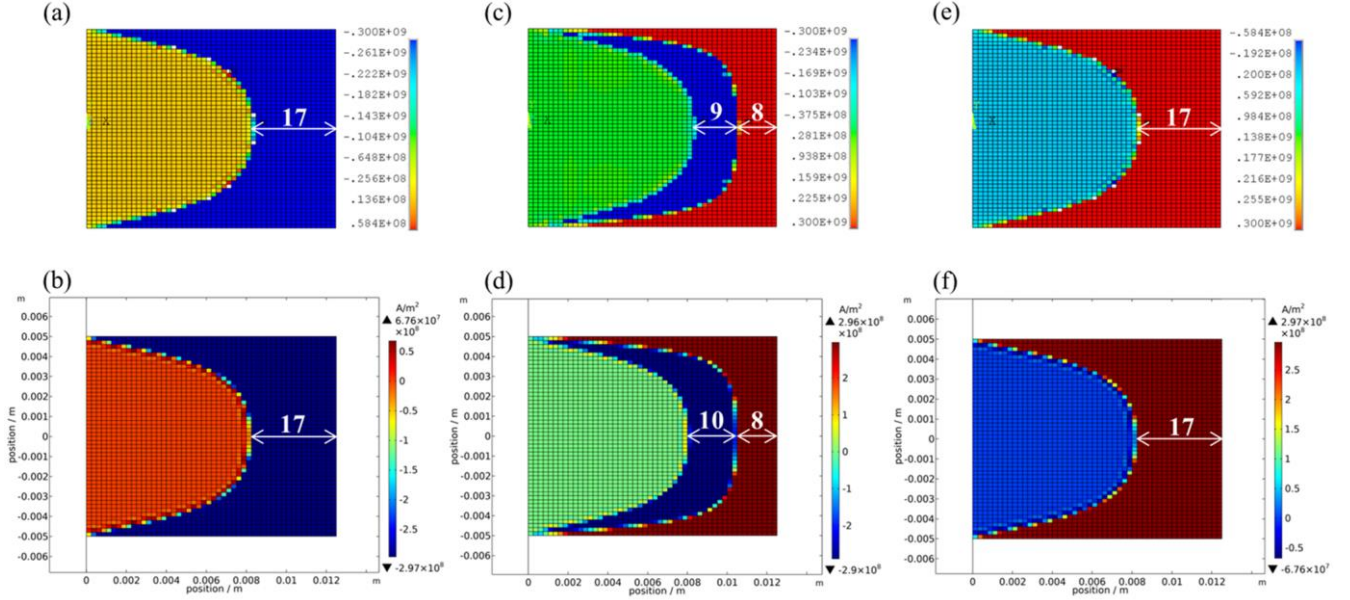


Figure 2. Trapped current density in ReBCO bulk (critical state model) after external magnetic field ascends linearly from zero to 1 T in 500 seconds by (a) using $A\cdot V\cdot A$ formula in ANSYS and (b) using H -formula in COMSOL. Trapped current density in ReBCO bulk after external magnetic field ascends linearly from zero to 1 T in 500 seconds and then descends linearly from 1 T to zero in another 500 seconds by (c) using $A\cdot V\cdot A$ formula in ANSYS and (d) using H -formula in COMSOL. Trapped current density in ReBCO bulk after FC magnetization from 1 T to zero in 500 seconds by (e) using $A\cdot V\cdot A$ formula in ANSYS and (f) using H -formula in COMSOL.

external magnetic field going through the ReBCO bulk is provided by controlling source current density of the solenoid.

In Figure 1 (b) the external field rises linearly from zero to 1 T in 500 seconds. The iterative algorithm to solve this critical state model based ZFC magnetization process ($B_0=1$ T, $T_1=500$ s, $N_1=200$) is developed and plotted in Figure 1 (c) by following

a) Create 2D axis-symmetrical half electromagnetic model and divide the field ascending process into N_1 load steps.

b) Apply an external field of B_0/N_1 at “ $t=T_1/N_1$ ” and solve this transient electromagnetic analysis as load step-1.

c) Extract the trapped current density (J_T) for each ReBCO bulk element after load step-1 and force J_T to $J_c \cdot J_T / |J_T|$ if the bulk element is over-trapped ($|J_T| \geq J_c$). This can be done by modifying their

element-type to ET-1 and using the “BFE” command to force their current density, meanwhile, making their eddy current solver inactive in future.

d) Set external field to $2B_0/N_1$ at “ $t=2T_1/N_1$ ” and solve this transient electromagnetic analysis as load step-2;

e) Do loop calculations for (c)-(d) by iterating i through 2 to N_1 . The final trapped J_T in ReBCO bulk can be reached after solving load step- N_1 .

Assuming J_c is constantly 3×10^8 A/m² the trapped J_T in ReBCO bulk is solved and plotted in Figure 2 (a). It can be found that all the penetrated ReBCO bulk elements carry a constant current density of -3×10^8 A/m² at “ $t=500$ s”. The penetration depth in the mid-plane is 17 bulk-elements (17 x 0.25 mm). In Figure 2 (b) the trapped J_T is solved by defining an n -value of 200 in COMSOL H -formula to approach the critical state model. The trapped J_T and the

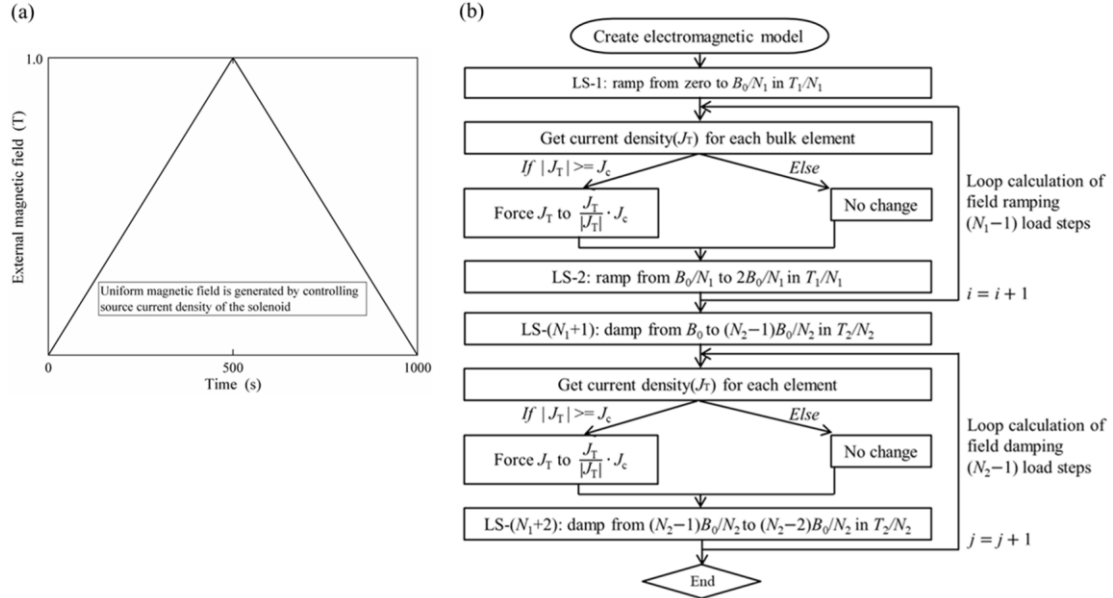


Figure 3. (a) ZFC magnetization - external magnetic field rises linearly from zero to 1 T in 500 seconds and then descends linearly from 1 T to zero in another 500 seconds; (b) Iterative algorithm method for simulating the critical state model based ZFC magnetization ($J_c=3\times 10^8$ A/m², $B_0=1$ T, $T_1=500$ s, $T_2=500$ s, $N_1=200$, $N_2=200$).

penetrating depth in ReBCO bulk are extremely close to those shown in Figure 2 (a).

2.2. ZFC magnetization - external field rises from zero to 1 T and then drops to zero

In Figure 3 (a) the external field going through the ReBCO bulk rises linearly from zero to 1 T in 500 seconds and then drops linearly to zero in another 500 seconds. The iterative algorithm for solving this critical state model based ZFC magnetization process is developed and plotted in Figure 3 (b) ($J_c=3\times 10^8$ A/m², $B_0=1$ T, $T_1=500$ s, $T_2=500$ s, $N_1=200$, $N_2=200$).

As described in Section-2.1, the element-type of the penetrated bulk elements after load step-200 has been modified to ET-1 in which the eddy current solver is inactive. So it is necessary to reset the element-type of the penetrated bulk elements to ET-2 to simulate the field descending process. However, the forced current density in the penetrated bulk elements will disappear because ET-2, with the freedom degree

of $\mathbf{A} \cdot \mathbf{V}$, cannot inherit the forced current density. A viable way to reserve the trapped J_T is to apply nodal voltages to the penetrated bulk elements. The applied nodal voltage for each penetrated bulk element fulfills

$$V = -2\pi \cdot r \cdot \rho_0 \cdot J_c \quad (4)$$

where r refers to the nodal radius (distance between the node and the central axis).

After installing the trapped J_T into ET-2 we start to simulate the critical state model based field descending process through following steps

- Set external field to $(N_2 - 1)B_0/N_2$ at “ $t=T_1+T_2/N_2$ ” and solve this transient electromagnetic analysis as load step-(N_1+1).
- Extract J_T for each ReBCO bulk element after load step-(N_1+1) and force J_T to $J_c \cdot J_T/|J_T|$ if $|J_T|$ is larger than J_c .
- Set external field to $(N_2 - 2)B_0/N_2$ at “ $t=T_1+2T_2/N_2$ ” and solve this transient electromagnetic analysis as load step-(N_1+2).
- Do loop calculations for (b)-(c) by iterating j

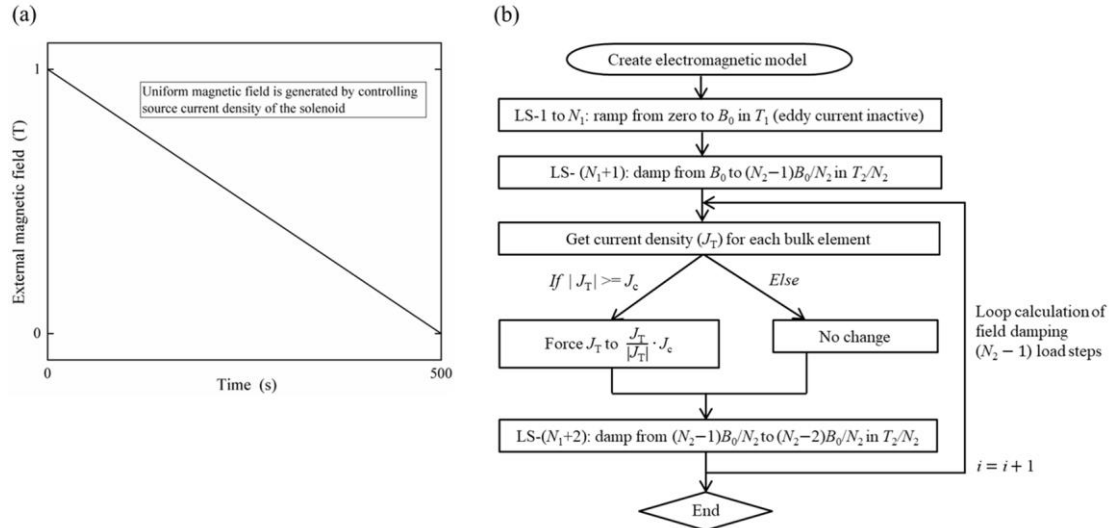


Figure 4. (a) FC magnetization - external magnetic field drops linearly from 1 T to zero in 500 seconds; (b) Iterative algorithm method for simulating the critical state model based FC magnetization ($J_c=3 \times 10^8$ A/m², $B_0=1$ T, $T_2=500$ s, $N_2=200$).

through 2 to N_2 . The final trapped J_T in ReBCO bulk can be reached after solving load step- (N_1+N_2) .

Figure 2 (c) and (d) compares the trapped J_T in ReBCO bulk through using ANSYS A-V-A formula and COMSOL H-formula. In Figure 2 (c) the ReBCO bulk traps 3×10^8 A/m² in the outer layer and -3×10^8 A/m² in the inner layer at “ $t=1000$ s”. The penetration depth is 8 bulk-elements (8 x 0.25 mm) for the outer layer and 9 bulk-elements (9 x 0.25 mm) for the inner layer. In Figure 2 (d) the ReBCO bulk traps $\sim 2.96 \times 10^8$ A/m² in the outer layer and $\sim -2.90 \times 10^8$ A/m² in the inner layer at “ $t=1000$ s”. The trapped $|J_T|$ is slightly lower than J_c because the flux creep effect cannot be eliminated entirely even for “ $n=200$ ”. This explains why the penetration depth of the inner layer is slightly larger than that shown in Figure 2 (c).

2.3. FC magnetization - field drops from 1 T to zero

For FC magnetization the temperature of ReBCO bulk is kept above T_c when external field rises from zero to B_0 . This step can be realized in ANSYS-IAM by

setting the element-type of ReBCO bulk to ET-1 and using the “BFE” command to force the current density to be zero. Then no eddy current will be generated in the ReBCO bulk during external magnetic field ascends.

When the ReBCO bulk becomes superconducting the external field drops linearly to zero as shown in Figure 4 (a). Details of the developed iterative algorithm for solving this critical state model based FC magnetization process ($J_c=3 \times 10^8$ A/m², $B_0=1$ T, $T_2=500$ s, $N_2=200$) are given in Figure 4 (b).

Figure 2 (e) and (f) compares the trapped J_T in ReBCO bulk through using ANSYS A-V-A formula and COMSOL H-formula. The simulation results are similar to those shown in Figure 2 (a) and (b) but with opposite current direction.

3. The flux creep model based iterative algorithm and its application in ZFC and FC magnetization

3.1. ZFC magnetization - external field rises from zero to 1 T

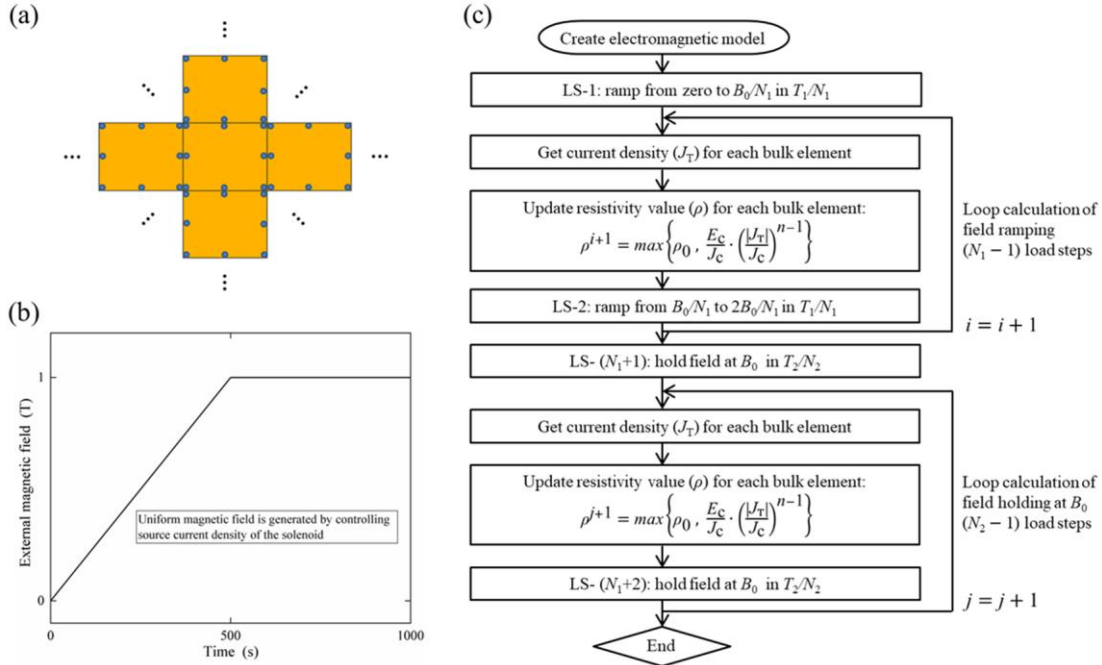


Figure 5. (a) Selected elements and nodes in the meshed ReBCO bulk; (b) ZFC magnetization - external magnetic field going through the ReBCO bulk rises linearly from zero to 1 T in 500 seconds and holds at 1 T for another 500 seconds; (c) Iterative algorithm method for simulating flux creep model based ZFC magnetization ($J_c=3\times 10^8$ A/m², $n=20$, $B_0=1$ T, $T_1=500$ s, $T_2=500$ s, $N_1=200$, $N_2=200$).

Similar to the FEA model shown in Figure 1 (a), the ReBCO bulk is meshed with ET-2 (*Plane233, A-V*) and non-superconductor areas are meshed with ET-1 (*Plane233, A*) for the flux creep model. But the meshed ReBCO bulk elements are separated with each other as shown in Figure 5 (a).

In Figure 5 (b) the external field going through the ReBCO bulk rises linearly from zero to 1 T in 500 seconds and holds at 1 T for another 500 seconds. The iterative algorithm for solving this flux creep model based ZFC magnetization process ($J_c=3\times 10^8$ A/m², $n=20$, $\rho_0=10^{-15}$ Ω·m, $B_0=1$ T, $T_1=500$ s, $T_2=500$ s, $N_1=200$, $N_2=200$) is developed and plotted in Figure 5 (c) by following

a) Create 2D axis-symmetrical half electromagnetic model in which ReBCO bulk elements are separated, having discontinuous nodes between each other.

b) Couple the freedom degree of A in the coincident nodes owned by neighboring bulk elements, therefore, ensuring a continuous solution results of the magnetic flux density.

c) Apply an external field of B_0/N_1 at “ $t=T_1/N_1$ ” and solve this transient electromagnetic analysis as load step-1.

d) Extract J_T for each ReBCO bulk element after load step-1.

e) Update the resistivity of each bulk element according to (5)

$$\rho^{i+1} = \max\left\{\rho_0, \frac{E_c}{J_c} \cdot \left(\frac{|J_T|}{J_c}\right)^{n-1}\right\} \quad (5)$$

f) Set external field to $2B_0/N_1$ at “ $t=2T_1/N_1$ ” and solve this transient electromagnetic analysis as load step-2.

g) Do loop calculations for (d)-(f) by iterating i through 2 to N_1 .

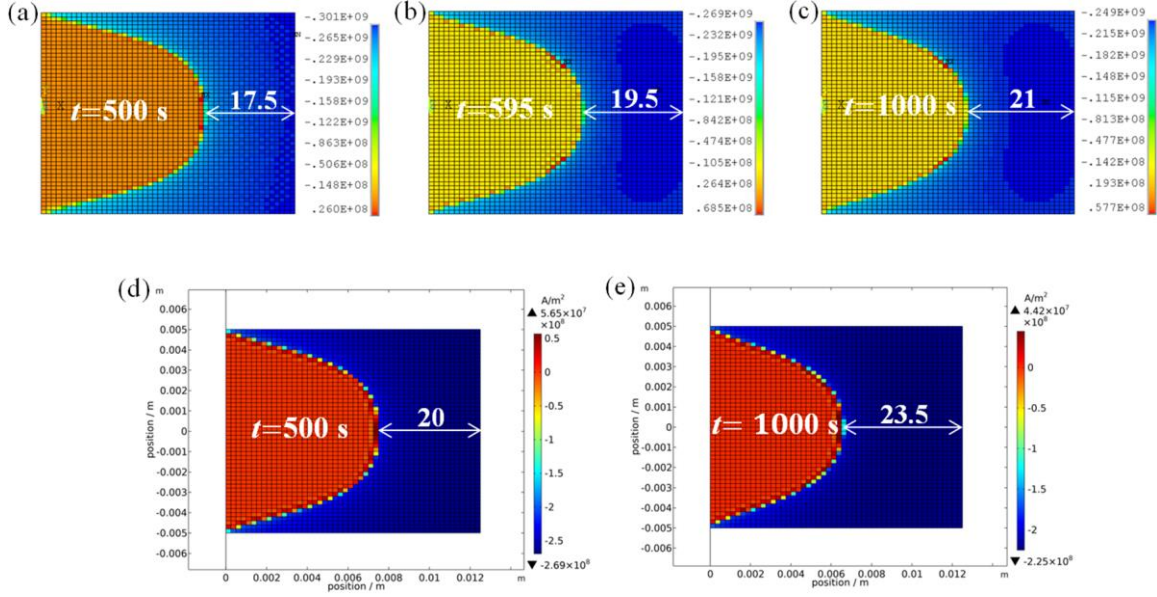


Figure 6. ANSYS A-V-A formula calculated J_T in ReBCO bulk at (a) $t=500$ s; (b) $t=595$ s; (c) $t=1000$ s. COMSOL H-formula calculated J_T in ReBCO bulk at (d) $t=500$ s; (e) $t=1000$ s. The external field for magnetization follows Figure 5 (a). n -value=20.

h) Hold external field at zero and do loop calculations by updating the resistivity of each bulk element after each load step.

The freedom degree of V in the coincident nodes owned by neighboring bulk elements is not coupled, thus, the neighboring ReBCO bulk elements can trap independent eddy current density without affecting each other. Specially, we shall eliminate abrupt J_T -drop during the loop calculation when insufficient load steps or large n -value is specified (the updated resistivity may jump). A viable way is to define a maximum drop ratio of J_T in each bulk element by setting nodal-voltage boundary according to (6)

$$V^{i+1} = 2\pi \cdot r \cdot \rho^{i+1} \cdot J_T \cdot (1 - F_d) \quad (6)$$

where F_d is named drop factor (maximum drop ratio) of J_T during loop calculation. The suggested F_d is 10%

for $n=20$ and 5% for larger n -value.

Figure 6 (a)-(c) plots the trapped J_T in ReBCO bulk at different time steps solved by using ANSYS A-V-A formula. The peak $|J_T|$ drops from 3.01×10^8 A/m² at “ $t=500$ s” to 2.69×10^8 A/m² at “ $t=595$ s” and then to 2.49×10^8 A/m² at “ $t=1000$ s” while the penetration depth in the mid-plane rises from 17.5 bulk-elements at “ $t=500$ s” to 19.5 bulk-elements at “ $t=595$ s” and then to 21 bulk-elements at “ $t=1000$ s”.

Figure 6 (d)-(e) plots the trapped J_T in ReBCO bulk at different time steps solved by using COMSOL H-formula. The peak trapped $|J_T|$ drops from 2.69×10^8 A/m² at “ $t=500$ s” to 2.25×10^8 A/m² at “ $t=1000$ s” while the penetration depth in the mid-plane rises from 20 bulk-elements at “ $t=500$ s” to 23.5 bulk-elements at “ $t=1000$ s”.

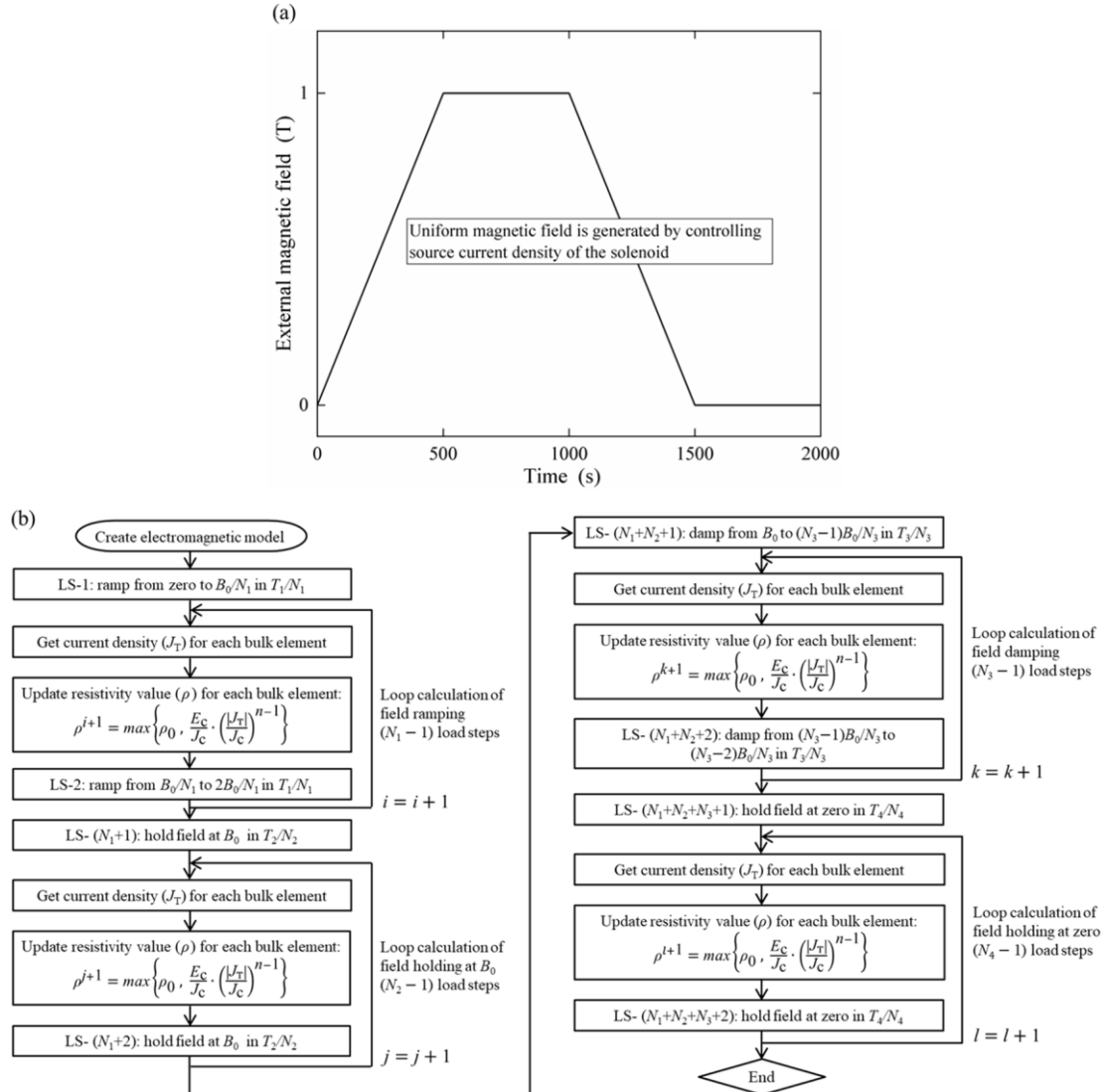


Figure 7. (a) ZFC magnetization - external magnetic field going through the ReBCO bulk rises linearly from zero to 1 T in 500 seconds and then holds at 1 T for 500 seconds and then drops linearly to zero in 500 seconds and then holds at zero for 500 seconds; (b) Iterative algorithm method for simulating flux creep model based ZFC magnetization ($J_c=3\times 10^8$ A/m², $n=20$, $B_0=1$ T, $T_1=500$ s, $T_2=500$ s, $T_3=500$ s, $T_4=500$ s, $N_1=200$, $N_2=200$, $N_3=200$, $N_4=200$).

By comparing the solution results from two different FEM software we find ~10% deviation of the simulation results both at “ $t=500$ s” and “ $t=1000$ s”. Specially, the trapped J_T at “ $t=595$ s” in Figure 6 (b) is in good agreement with the trapped J_T at “ $t=500$ s” in Figure 6 (d). This indicates the ReBCO bulk solved by two different FEM software traps the same electromagnetic energy after the field ramping. Assuming there is no energy loss (joule heating effect) during J_T ’s relaxation we can expect to get the same

trapped current profile in the ReBCO bulk after holding for a considerable length of time.

3.2. ZFC magnetization - external field rises from zero to 1 T and then drops to zero

In Figure 7 (a) the external field going through the ReBCO bulk rises linearly from zero to 1 T in 500 seconds and holds at 1 T for 500 seconds, and then drops linearly to zero in 500 seconds and holds at zero for 500 seconds. The iterative algorithm for solving this flux creep model based ZFC magnetization

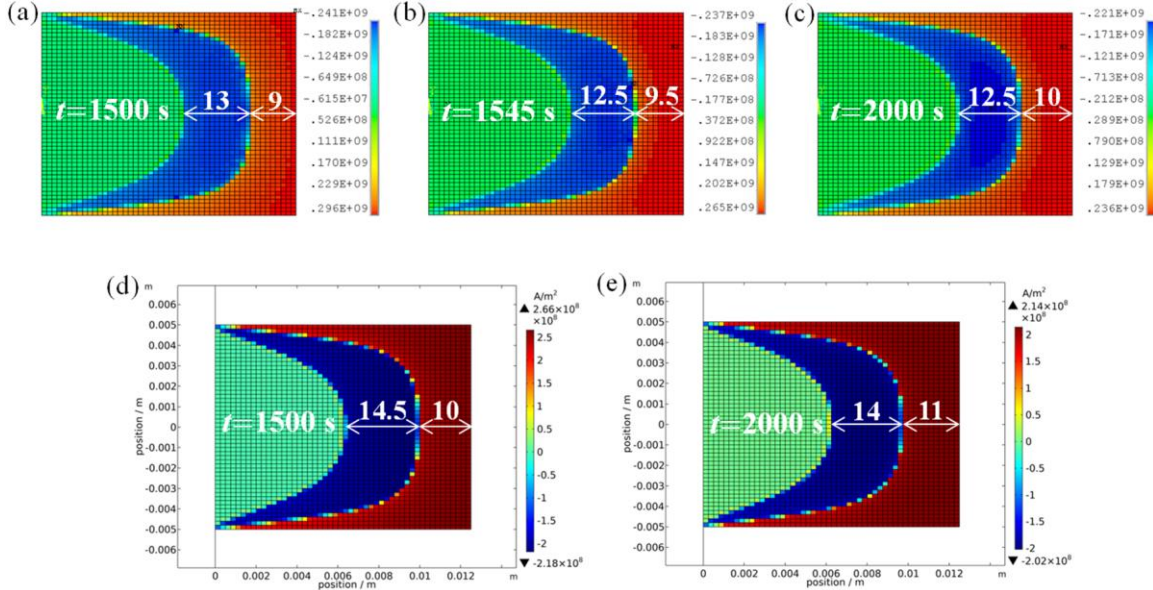


Figure 8. ANSYS A-V-A formula calculated J_T in ReBCO bulk at (a) $t=1500$ s; (b) $t=1545$ s; (c) $t=2000$ s. COMSOL H-formula calculated J_T in ReBCO bulk at (d) $t=1500$ s; (e) $t=2000$ s. The external field for magnetization follows Figure 7 (a). n -value=20.

process is developed and plotted in Figure 7 (b) ($J_c=3\times 10^8$ A/m², $n=20$, $B_0=1$ T, $T_1=500$ s, $T_2=500$ s, $T_3=500$ s, $T_4=500$ s, $N_1=200$, $N_2=200$, $N_3=200$, $N_4=200$). The left iterative part for the field's ascending and holding process is the same as that shown in Figure 5 (c). The right iterative part, quite similar to the left, is added to simulate the field's descending and holding process. Likewise we need to update the element resistivity and restrain the drop rate of J_T in each bulk element after each load step electromagnetic analysis.

Figure 8 (a)-(c) plots the trapped J_T in ReBCO bulk at different time steps solved by using ANSYS A-V-A formula. For the outer trapped layer the peak $|J_T|$ drops from 2.96×10^8 A/m² at “ $t=1500$ s” to 2.65×10^8 A/m² at “ $t=1545$ s” and then to 2.36×10^8 A/m² at “ $t=2000$ s” while the penetration depth in the mid-plane rises from 9 bulk-elements at “ $t=1500$ s” to 9.5 bulk-elements at “ $t=1545$ s” and then to 10 bulk-elements at “ $t=2000$ s”. For the inner trapped

layer the peak $|J_T|$ drops from 2.41×10^8 A/m² at “ $t=1500$ s” to 2.37×10^8 A/m² at “ $t=1545$ s” and then to 2.21×10^8 A/m² at “ $t=2000$ s” while the penetration depth in the mid-plane is slightly eaten by the outer layer from “ $t=1500$ s” to “ $t=2000$ s”.

Figure 8 (d)-(e) plots the trapped J_T in ReBCO bulk at different time steps solved by using COMSOL H-formula. For the outer trapped layer the peak $|J_T|$ drops from 2.66×10^8 A/m² at “ $t=1500$ s” to 2.14×10^8 A/m² at “ $t=2000$ s” while the penetration depth in the mid-plane rises from 10 bulk-elements at “ $t=1500$ s” to 11 bulk-elements at “ $t=2000$ s”. For the inner trapped layer the peak $|J_T|$ drops from 2.18×10^8 A/m² at “ $t=1500$ s” to 2.02×10^8 A/m² at “ $t=2000$ s” while the penetration depth in the mid-plane is slightly eaten by the outer layer from “ $t=1500$ s” to “ $t=2000$ s”.

Specially, the trapped J_T of the outer layer at “ $t=1545$ s” in Figure 8 (b) is in good agreement with the trapped J_T of the outer layer at “ $t=1500$ s” in Figure 8 (d).

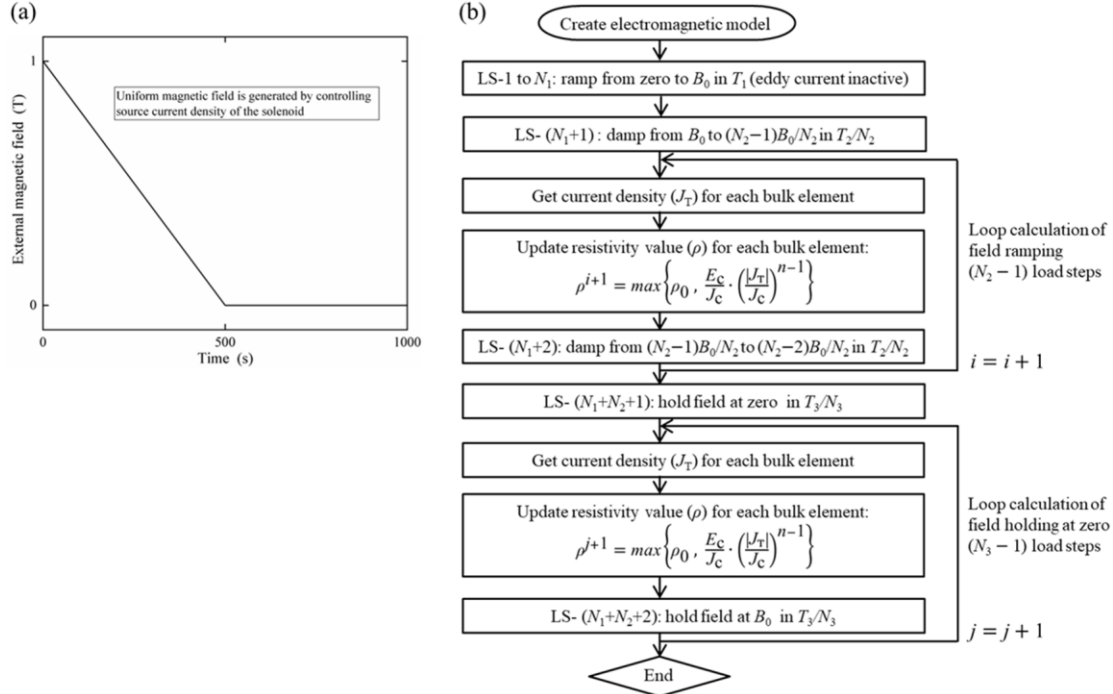


Figure 9. (a) FC magnetization - external magnetic field going through the ReBCO bulk drops linearly from 1 T to zero in 500 seconds and then holds at zero for another 500 seconds; (b) Iterative algorithm method for simulating flux creep model based FC magnetization ($J_c=3 \times 10^8$ A/m², $n=20$, $B_0=1$ T, $T_2=500$ s, $T_3=500$ s, $N_2=200$, $N_3=200$).

3.3. FC magnetization - field drops from 1 T to zero

No eddy current will be generated in the ReBCO bulk ($T > T_c$) during external field rises from zero to 1 T. This can be realized by using the method suggested in [Section-2.3](#). When the ReBCO bulk becomes superconducting and external field descends we start to simulate the magnetization current by referring to [Figure 9 \(a\) and \(b\)](#).

[Figure 10 \(a\)-\(e\)](#) plots the trapped J_T in ReBCO bulk solved by using ANSYS A-V-A formula and

COMSOL H -formula. The simulation results are similar to those shown in [Figure 6 \(a\)-\(e\)](#) but with opposite current direction.

All above simulations for the flux creep model assume n -value equals to 20 and set the drop factor F_d to 10%. It is often more time-consuming or sometimes hard to converge when solving large n -value based magnetization problems in COMSOL. By using ANSYS-IAM we can also meet troubles like “continuous resistivity jump”. This problem can be solved by defining a small drop factor F_d (for example, 5% for $n=40$).

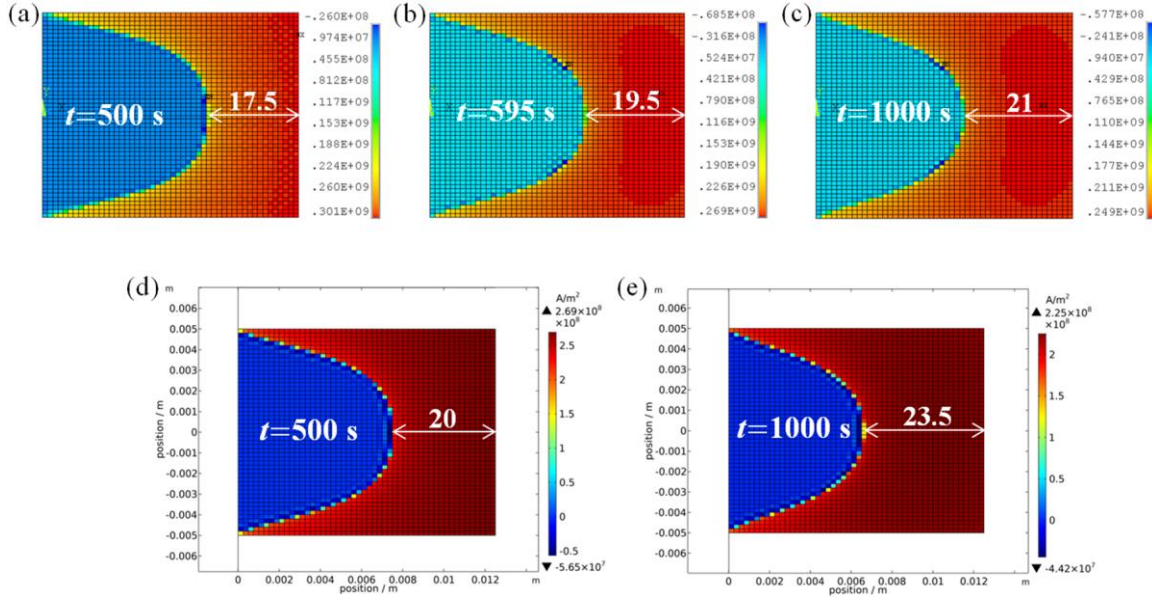


Figure 10. ANSYS A-V-A formula calculated J_T in ReBCO bulk at (a) $t=500$ s; (b) $t=595$ s; (c) $t=1000$ s. COMSOL H-formula calculated J_T in ReBCO bulk at (d) $t=500$ s; (e) $t=1000$ s. The external field for magnetization follows Figure 9 (a). n -value=20.

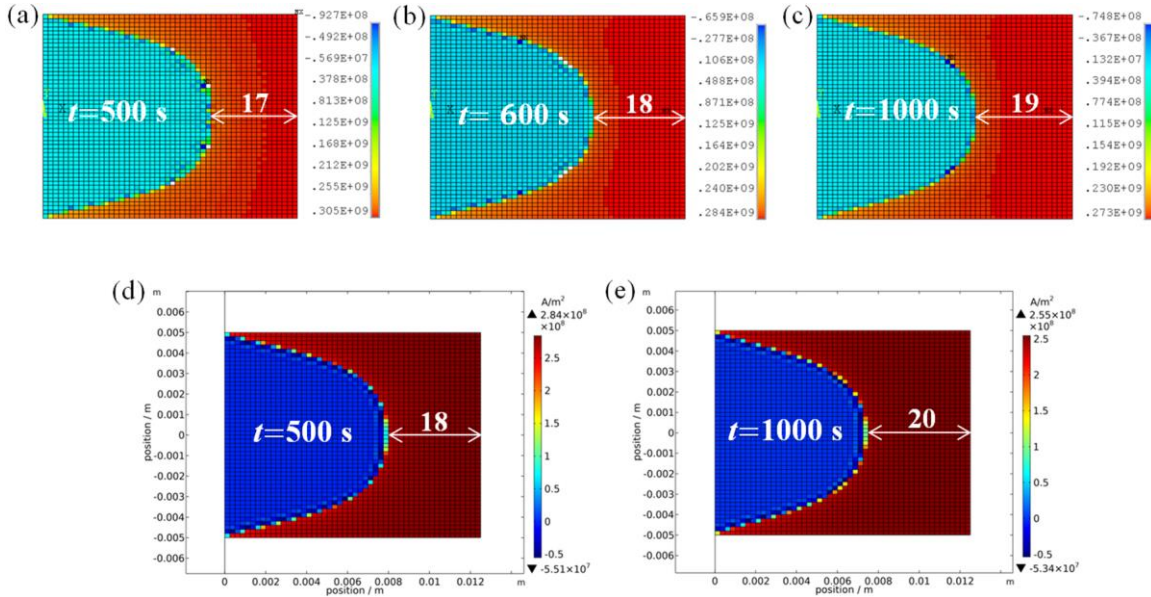


Figure 11. ANSYS A-V-A formula calculated J_T in ReBCO bulk at (a) $t=500$ s; (b) $t=600$ s; (c) $t=1000$ s. COMSOL H-formula calculated J_T in ReBCO bulk at (d) $t=500$ s; (e) $t=1000$ s. The external field for magnetization follows Figure 5 (a). n -value=40.

Figure 11 (a)-(c) plots the trapped J_T in ReBCO bulk when we set the n -value to 40 in ANSYS-IAM and damp external field as shown in Figure 9 (a). The peak J_T drops from 3.05×10^8 A/m² at “ $t=500$ s” to 2.84×10^8 A/m² at “ $t=600$ s” and then to 2.73×10^8 A/m²

at “ $t=1000$ s” while the penetration depth in the mid-plane rises from 17 bulk-elements at “ $t=500$ s” to 18 bulk-elements at “ $t=600$ s” and then to 19 bulk-elements at “ $t=1000$ s”. Figure 11 (d)-(e) plots the trapped J_T in ReBCO bulk solved by using

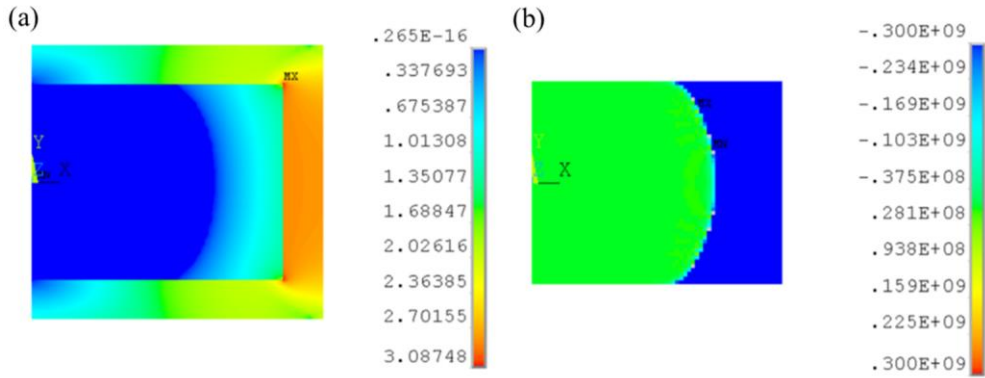


Figure 12. (a) Trapped magnetic field in ReBCO bulk and iron; (b) Trapped current density in ReBCO bulk. The external magnetic field ascends linearly from zero to 1 T in 500 seconds (critical state model).

COMSOL \mathbf{H} -formula. The peak J_T drops from 2.84×10^8 A/m² at “ $t=500$ s” to 2.55×10^8 A/m² at “ $t=1000$ s” while the penetration depth in the mid-plane rises from 18 bulk-elements at “ $t=500$ s” to 20 bulk-elements at “ $t=1000$ s”. By comparing the solution results from two different FEM software we find ~5% deviation of the penetrating depth both at “ $t=500$ s” and “ $t=1000$ s”. Specially, we find the trapped J_T at “ $t=500$ s” in Figure 11 (d) is in good agreement with the trapped J_T at “ $t=600$ s” in Figure 11 (b).

4. Implement B - H , $J_c(B)$ and $J_c(\varepsilon)$ into the magnetization process

In this section the possibility of implementing B - H , $J_c(B)$ and $J_c(\varepsilon)$ into the magnetization process is investigated by “repeating” the simulation in Section-2.1.

4.1. Trapped J_T in ReBCO bulk when including ferromagnetic materials

Simulation or experimental studies show that ferromagnetic materials encompassing the bulk superconductors can help to increase the trapped magnetic field in the whole system [39, 55]. It is therefore interesting to check the feasibility of adding

ferromagnetic materials into the ANSYS model. To achieve this we re-run the simulation case after modifying Air-1 in Figure 1 (a) to B - H curve based ferromagnetic iron.

Figure 12 (a) plots the trapped magnetic field in ReBCO bulk and ferromagnetic iron after external field rises to 1 T. The peak magnetic field reaches ~3 T in the iron. Figure 12 (b) plots the trapped J_T in ReBCO bulk where we find the penetration depth is much smaller than that shown in Figure 2 (a). This is because the magnetic flux lines going through the ReBCO bulk are partially taken away by the iron. The iron shares the task with the ReBCO bulk to fight against the ascending of external magnetic field.

4.2. Trapped J_T in ReBCO bulk when considering J_c - B dependence

For practical high T_c superconductors the relation between critical current density and magnetic field can be described by Kim model [47, 56-57]. It is often necessary to take into account the J_c - B dependence for a ZFC magnetization process. Here we assume the critical current density of ReBCO bulk material fulfills

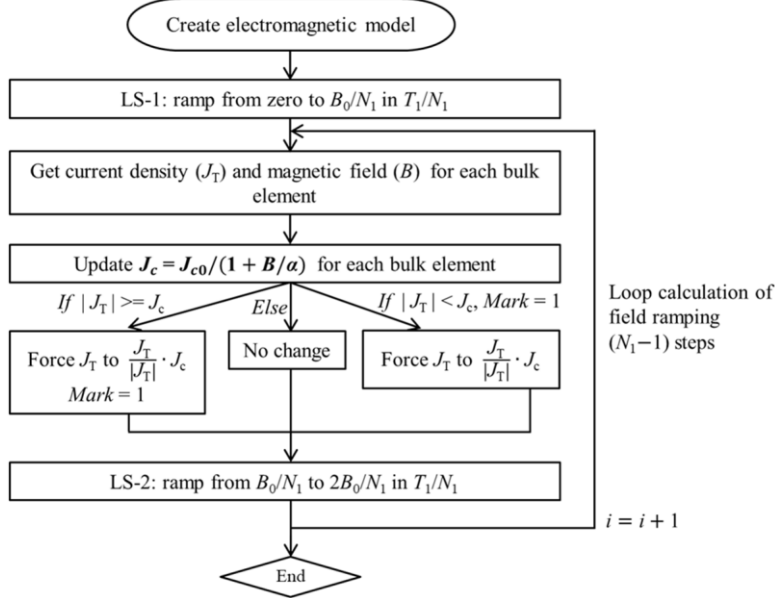


Figure 13. Iterative algorithm for magnetization simulation when considering J_c - B dependence ($J_{c0}=3\times 10^8$ A/m², $\alpha=1$ T, $B_0=1$ T, $T_1=500$ s, $N_1=200$).

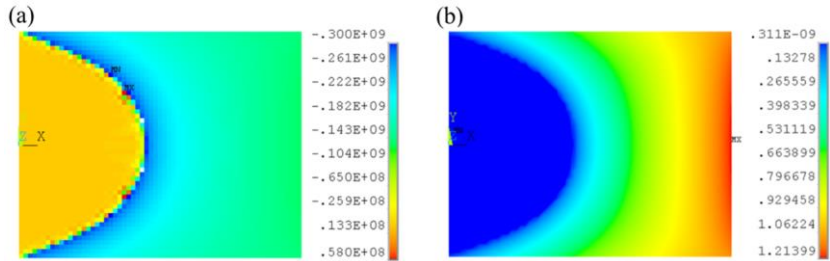


Figure 14. (a) Trapped current density in the ReBCO bulk; (b) Magnetic field map in the ReBCO bulk. The external magnetic field ascends linearly from zero to 1 T in 500 seconds.

$$J_c = J_{c0}/(1 + B/\alpha) \quad (7)$$

where α is 1 T and J_{c0} is 3×10^8 A/m².

The iterative algorithm for solving the J_c - B dependent and critical state model based ZFC magnetization process is developed and plotted in Figure 13. Specially, we need to extract the magnetic field B of each ReBCO bulk element and update the J_c according to (7) after solving each load step. If the trapped $|J_T|$ for the i^{th} bulk element is larger than J_c we modify the element-type of the i^{th} bulk element to ET-1 and use “BFE” command to force the trapped J_T to $J_c \cdot J_T / |J_T|$. In addition, the bulk elements who are not penetrated are marked as “ $mark = 0$ ” and the bulk

elements who have ever been penetrated are marked as “ $mark = 1$ ”. If $|J_T|$ for the i^{th} bulk element is smaller than J_c and the i^{th} bulk element has been penetrated before ($mark = 1$) we will use “BFE” command to force the trapped J_T to the updated $J_c \cdot J_T / |J_T|$.

Figure 14 (a) and (b) plots the trapped J_T and the magnetic field in ReBCO bulk after external field rises to 1 T. It is as well as expected that the higher magnetic field region traps a lower $|J_T|$ in the whole ReBCO bulk. The relation between the trapped current density (absolute value) and the magnetic field in each bulk element satisfies (7) perfectly.

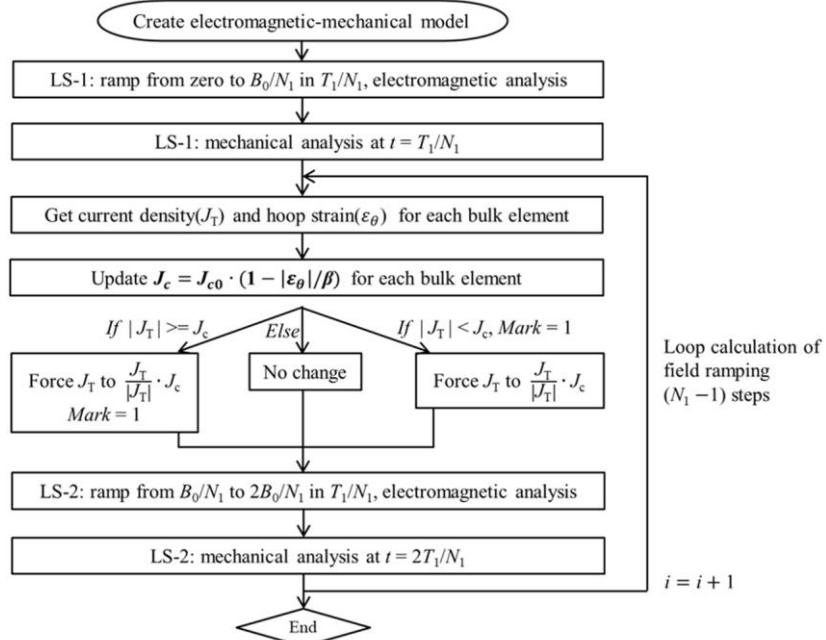


Figure 15. Iterative algorithm for magnetization simulation when considering J_c - ε dependence ($J_{c0}=3\times10^8$ A/m², $\beta=1.5\times10^{-5}$, $B_0=1$ T, $T_1=500$ s, $N_1=200$).

4.3. Trapped J_T in ReBCO bulk when considering J_c - ε dependence

Extensive studies on the relation between critical current and strain (or stress) have been carried out for commercial HTS wires or cables [58-62]. Compared to brittle Bi-2212 round wire [63-64] after heat treatment, ReBCO tape is with excellent mechanical property as the Hastelloy substrate can share the major tensile or compressive stress. This feature makes commercial ReBCO tape attractive to be used to reach a magnetic field above 20 T [65-69]. For practical ReBCO bulk materials there still lacks a scaling law for J_c - ε under varied magnetic field. However, recent work, towards pushing the trapped magnetic field in disk-shaped ReBCO bulk, indicates there is an obvious J_c reduction at high magnetic field because of the large stress level induced by Lorentz force [37]. It is therefore necessary to take into account the J_c - ε dependence when simulating high field magnetization process.

Here we attempt to confirm the feasibility of adding J_c - ε dependence into ANSYS-IAM by assuming the critical current density of ReBCO bulk material fulfills

$$J_c = \left(1 - \frac{|\varepsilon_\theta|}{\beta}\right) J_{c0} \quad (8)$$

where β is 1.5×10^{-5} , J_{c0} is 3×10^8 A/m² and ε_θ refers to hoop strain.

The iterative algorithm for solving the J_c - ε dependent and critical state model based ZFC magnetization process is developed and plotted in Figure 15. After transient electromagnetic analysis of load step-1 we perform static mechanical analysis by switching the electromagnetic element-type of *Plane233* to the structural element-type of *Plane183* and importing the Lorentz force data to the mechanical model. After the static mechanical analysis of load step-1 we extract the hoop strain ε_θ of each bulk element, update the J_c according to (8) and switch the element-type back to *Plane233* for electromagnetic analysis of the next load step. This

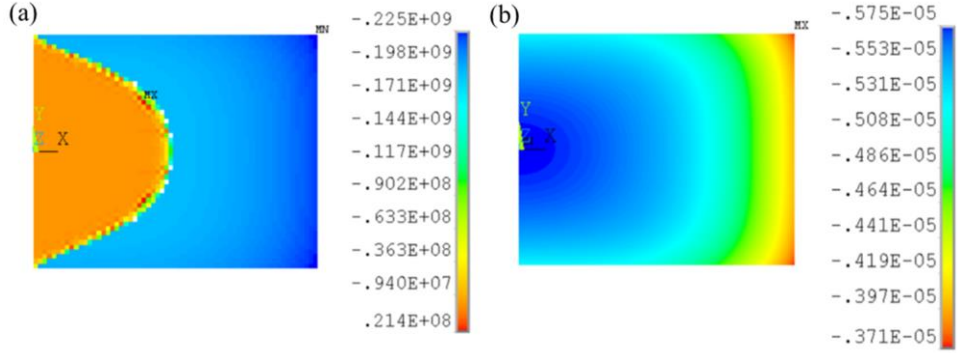


Figure 16. (a) Trapped current density in the ReBCO bulk; (b) Hoop strain in the ReBCO bulk. The external magnetic field ascends linearly from zero to 1 T in 500 seconds.

iterative algorithm is quite similar to that shown in Figure 13.

Figure 16 (a) and (b) plots the trapped J_T and the hoop strain in ReBCO bulk after external field rises to 1 T. It is as well as expected that the lower $|\varepsilon_\theta|$ region traps higher $|J_T|$ in the whole ReBCO bulk. The relation between the trapped current density (absolute value) and the hoop strain in each bulk element satisfies (8) perfectly.

All above simulations in Section-4 are carried out for the critical state model. For flux creep model we can also implement B - H , $J_c(B)$ and $J_c(\varepsilon)$ into the magnetization process by using similar iterative algorithm method.

5. Discussion

To further understand the mechanism behind A - V - A formula based IAM we repeat the simulation case shown in Section-2.1 (critical state model, $J_c=3\times 10^8$ A/m²) and the simulation case in Section-3.1 (flux creep model, $J_c=3\times 10^8$ A/m², $n=20$) by defining different load steps (N_1), different initial resistivity (ρ_0)

for ReBCO bulk and different ramping time (T_1). The calculation stops after external magnetic field rises to 1 T at “ $t=T_1$ ”.

5.1. The critical state model

5.1.1. Number of specified load steps – N_1

Figure 17 compares the trapped J_T in ReBCO bulk at “ $t=T_1$ ” under varied simulation cases solved by critical state model. As shown in Figure 17 (a)-(d), the ReBCO bulk, penetrated with a constant J_T of -3×10^8 A/m², holds the same current-penetrating depth when we specify different iterative load steps ($\rho_0 = 10^{-16}$ Ω·m, $T_1 = 500$ s). But we can find several abnormal bulk elements (skipped in the contour) nearby the penetration boundary in Figure 17 (a) and (b) due to the lack of enough load steps. This is because these elements are over-magnetized and their J_T cannot be corrected after solving the final load step. Higher solution accuracy can be achieved when we specify more load steps for the magnetization process.

5.1.2. Initial resistivity – ρ_0

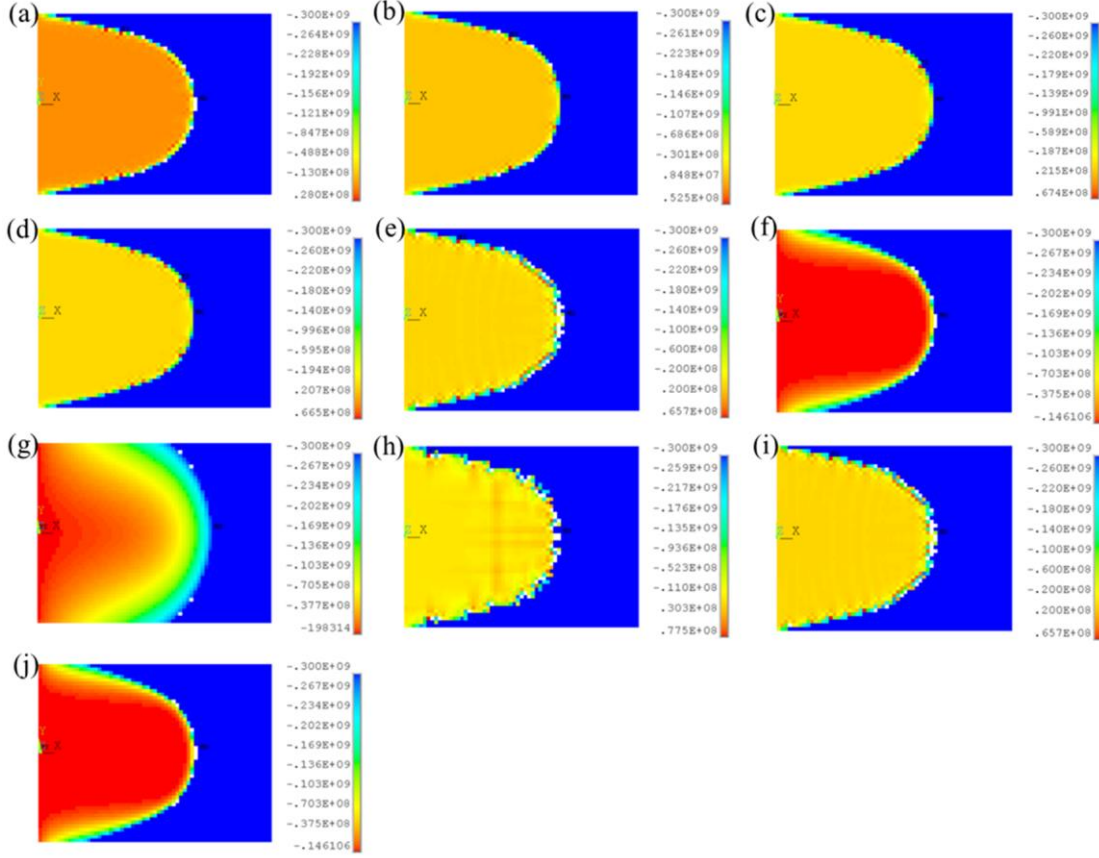


Figure 17. Trapped current density in the ReBCO bulk (critical state model) after external magnetic field rises to 1 T at (a) $\rho_0 = 10^{-16} \Omega \cdot \text{m}$, $T_1 = 500$ s, $N_1 = 100$; (b) $\rho_0 = 10^{-16} \Omega \cdot \text{m}$, $T_1 = 500$ s, $N_1 = 200$; (c) $\rho_0 = 10^{-16} \Omega \cdot \text{m}$, $T_1 = 500$ s, $N_1 = 500$; (d) $\rho_0 = 10^{-16} \Omega \cdot \text{m}$, $T_1 = 500$ s, $N_1 = 1000$; (e) $\rho_0 = 10^{-17} \Omega \cdot \text{m}$, $T_1 = 500$ s, $N_1 = 200$; (f) $\rho_0 = 10^{-15} \Omega \cdot \text{m}$, $T_1 = 500$ s, $N_1 = 200$; (g) $\rho_0 = 10^{-14} \Omega \cdot \text{m}$, $T_1 = 500$ s, $N_1 = 200$; (h) $\rho_0 = 10^{-16} \Omega \cdot \text{m}$, $T_1 = 5$ s, $N_1 = 200$; (i) $\rho_0 = 10^{-16} \Omega \cdot \text{m}$, $T_1 = 50$ s, $N_1 = 200$; (j) $\rho_0 = 10^{-16} \Omega \cdot \text{m}$, $T_1 = 5000$ s, $N_1 = 200$.

Figure 17 (b) and (e)-(g) compares the trapped current density in ReBCO bulk when we assign varied ρ_0 to ReBCO bulk ($N_1 = 200$, $T_1 = 500$ s). Compared to Figure 17 (b) who sets ρ_0 to $10^{-16} \Omega \cdot \text{m}$ we can find the same current-penetrating depth but more abnormal bulk elements nearby the penetration boundary in Figure 17 (e) who sets ρ_0 to $10^{-17} \Omega \cdot \text{m}$. In both Figure 17 (f) and (g) the ReBCO bulk ($\rho_0 = 10^{-15} \Omega \cdot \text{m}$ and $\rho_0 = 10^{-14} \Omega \cdot \text{m}$), however, is not well penetrated as expected. This indicates low ρ_0 can reduce the solution accuracy while high ρ_0 can impede the current penetrating process. Thus we need to take care

in selecting appropriate ρ_0 to simulate the magnetization process.

5.1.3. Ramping time – T_1

Figure 17 (b) and (h)-(j) compares the trapped current density in ReBCO bulk when we specify varied ramping time ($\rho_0 = 10^{-16} \Omega \cdot \text{m}$, $N_1 = 200$). Compared to Figure 17 (b) who sets T_1 to 500 s we can find the same current-penetrating depth but more abnormal bulk elements nearby the penetration boundary in either Figure 17 (h) or (i) who sets T_1 to 5 s or 50 s. In Figure 13 (j) the ReBCO bulk ($T_1 = 5000$ s), however, is not well penetrated as expected because of the low ramping rate.

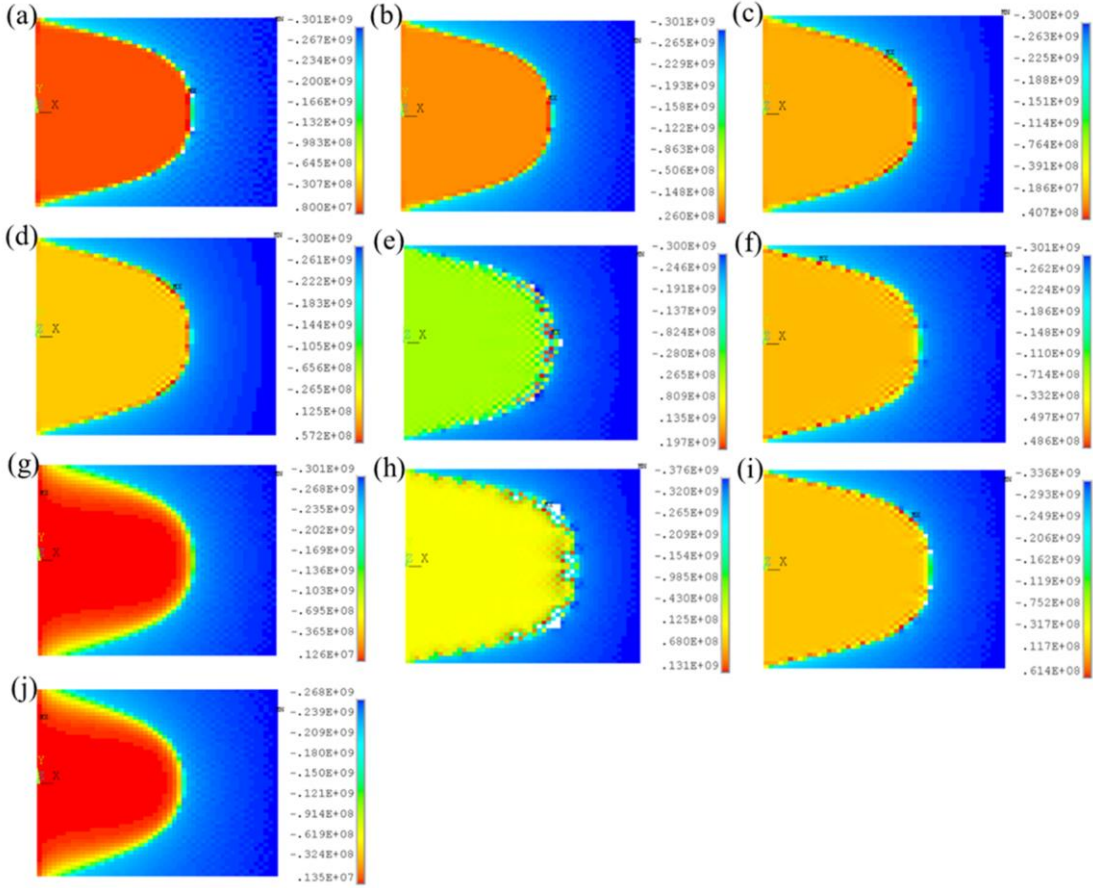


Figure 18. Trapped current density in the ReBCO bulk (flux creep model, $n = 20$) after external magnetic field rises to 1 T at (a) $\rho_0 = 10^{-15}\Omega\cdot m$, $T_1 = 500$ s, $N_1 = 100$; (b) $\rho_0 = 10^{-15}\Omega\cdot m$, $T_1 = 500$ s, $N_1 = 200$; (c) $\rho_0 = 10^{-15}\Omega\cdot m$, $T_1 = 500$ s, $N_1 = 500$; (d) $\rho_0 = 10^{-15}\Omega\cdot m$, $T_1 = 500$ s, $N_1 = 1000$; (e) $\rho_0 = 10^{-17}\Omega\cdot m$, $T_1 = 500$ s, $N_1 = 200$; (f) $\rho_0 = 10^{-16}\Omega\cdot m$, $T_1 = 500$ s, $N_1 = 200$; (g) $\rho_0 = 10^{-14}\Omega\cdot m$, $T_1 = 500$ s, $N_1 = 200$; (h) $\rho_0 = 10^{-15}\Omega\cdot m$, $T_1 = 5$ s, $N_1 = 200$; (i) $\rho_0 = 10^{-15}\Omega\cdot m$, $T_1 = 50$ s, $N_1 = 200$; (j) $\rho_0 = 10^{-15}\Omega\cdot m$, $T_1 = 5000$ s, $N_1 = 200$.

When the ReBCO bulk is in superconducting state the practical resistivity is zero, far below $10^{-16}\Omega\cdot m$. This means even a quite low ramping rate can generate a large eddy current density easily to penetrate the ReBCO bulk elements. We can re-assign

a smaller ρ_0 to ReBCO bulk when we meet the situation in Figure 17 (f)-(g) and (j). For critical state model the trapped current density in ReBCO bulk is independent of the ramping time during ZFC and FC magnetization.

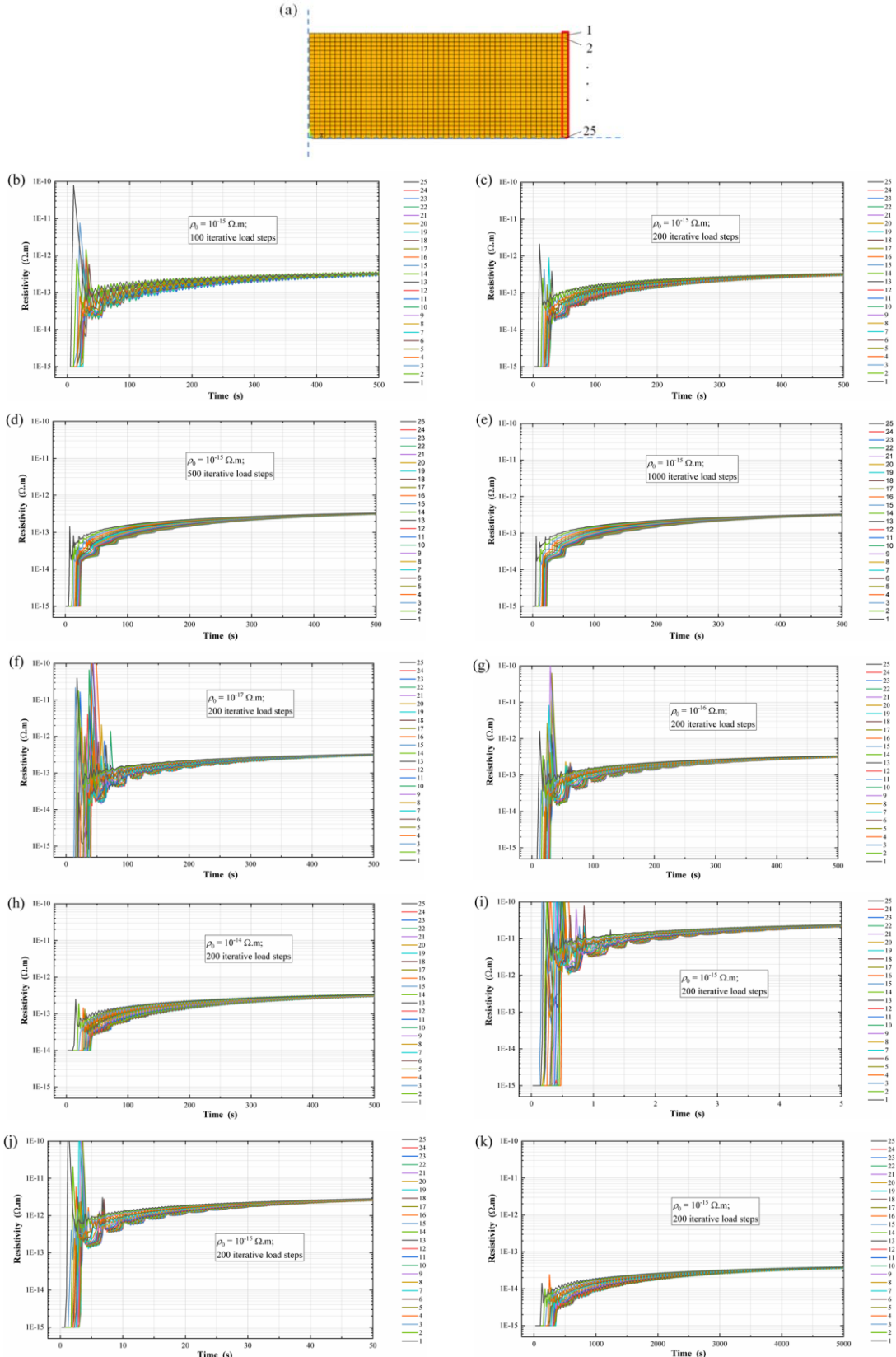


Figure 19. Resistivity evolution of (a) selected bulk elements during external field rises to 1 T (flux creep model, $n = 20$) at (b) $\rho_0 = 10^{-15} \Omega.m$, $T_1 = 500$ s, $N_1 = 100$; (c) $\rho_0 = 10^{-15} \Omega.m$, $T_1 = 500$ s, $N_1 = 200$; (d) $\rho_0 = 10^{-15} \Omega.m$, $T_1 = 500$ s, $N_1 = 500$; (e) $\rho_0 = 10^{-15} \Omega.m$, $T_1 = 500$ s, $N_1 = 1000$; (f) $\rho_0 = 10^{-17} \Omega.m$, $T_1 = 500$ s, $N_1 = 200$; (g) $\rho_0 = 10^{-16} \Omega.m$, $T_1 = 500$ s, $N_1 = 200$; (h) $\rho_0 = 10^{-14} \Omega.m$, $T_1 = 500$ s, $N_1 = 200$; (i) $\rho_0 = 10^{-15} \Omega.m$, $T_1 = 5$ s, $N_1 = 200$; (j) $\rho_0 = 10^{-15} \Omega.m$, $T_1 = 50$ s, $N_1 = 200$; (k) $\rho_0 = 10^{-15} \Omega.m$, $T_1 = 5000$ s, $N_1 = 200$.

5.2. The flux creep model

5.2.1. Number of specified load steps – N

Figure 18 compares the trapped current density in ReBCO bulk at “ $t=T_1$ ” under varied simulation cases solved by flux creep model ($n = 20$, $F_d = 10\%$). As shown in Figure 18 (a)-(d), the ReBCO bulk, with the same current-penetrating depth, traps similar current density when we specify different iterative load steps ($\rho_0 = 10^{-15} \Omega \cdot \text{m}$, $T_1 = 500 \text{ s}$). But we can find several abnormal bulk elements nearby the penetrating boundary in Figure 18 (a) due to lack of enough load steps.

The resistivity value of the marked 25 bulk elements in 2D half axis-symmetric FEA model, shown in Figure 19 (a), is extracted for all load steps. Take element-1 as an example, the resistivity shown in Figure 19 (b) jumps to $7.8 \times 10^{-11} \Omega \cdot \text{m}$ at load step-2, then calms down after load step-6 and finally “stabilizes” at $\sim 3.3 \times 10^{-13} \Omega \cdot \text{m}$; the resistivity shown in Figure 19 (c) jumps to $2.1 \times 10^{-12} \Omega \cdot \text{m}$ at load step-4, then calms down after load step-18 and finally “stabilizes” at $\sim 3.3 \times 10^{-13} \Omega \cdot \text{m}$; the resistivity shown in Figure 19 (d) jumps to $1.4 \times 10^{-13} \Omega \cdot \text{m}$ at load step-7, then calms down after load step-30 and finally “stabilizes” at $\sim 3.3 \times 10^{-13} \Omega \cdot \text{m}$; the resistivity shown in Figure 19 (e) jumps to $8.1 \times 10^{-14} \Omega \cdot \text{m}$ at load step-12, then calms down after load step-60 and finally “stabilizes” at $\sim 3.3 \times 10^{-13} \Omega \cdot \text{m}$. These calculation results indicate lots of iterative load steps can eliminate resistivity jump significantly but will not affect the final simulation results.

5.2.2. Initial resistivity – ρ_0

Figure 18 (b) and (e)-(g) compares the trapped current density in ReBCO bulk when we assign varied ρ_0 to ReBCO bulk ($N_1=200$, $T_1=500 \text{ s}$). Compared to Figure

18 (b) who sets ρ_0 to $10^{-15} \Omega \cdot \text{m}$ we can find quite similar simulation results in either Figure 18 (e) or (f) who sets ρ_0 to $10^{-17} \Omega \cdot \text{m}$ or $10^{-16} \Omega \cdot \text{m}$ but a few abnormal bulk elements nearby the penetration boundary in Figure 18 (e). In Figure 18 (g) the ReBCO bulk ($\rho_0 = 10^{-14} \Omega \cdot \text{m}$), however, is not well penetrated as expected. Similar to the critical state model, it is necessary to make a compromise in selecting appropriate ρ_0 to simulate the flux creep model based magnetization process.

Figure 19 (c) and (f)-(h) compares the development of resistivity of the marked 25 bulk elements when we assign varied ρ_0 to the ReBCO bulk. It can be found that the plotted resistivity values jump more quickly and oscillate longer when smaller ρ_0 is specified. Similar to Figure 19 (b)-(e) the final retained resistivity in element-1 is $\sim 3.3 \times 10^{-13} \Omega \cdot \text{m}$ in Figure 19 (f)-(h).

5.2.3. Ramping time – T_1

Unlike the critical state model the ramping time plays an important role in flux creep model based magnetization process. Figure 18 (b) and (h)-(j) compares the trapped current density in ReBCO bulk when we specify different ramping time ($\rho_0 = 10^{-15} \Omega \cdot \text{m}$, $N_1=200$). It can be found that the current-penetrating depth is larger and the peak $|J_T|$ is lower when a larger ramping time is defined. This is because large ramping time provides opportunities for the flux creep effects to relax the trapped current density [37, 47].

Figure 19 (c) and (i)-(k) compares the development of resistivity of the marked 25 bulk elements when we specify different ramping time. It

can be found that the plotted resistivity values jump more quickly, oscillate longer and finally “stabilize” at a larger value when shorter ramping time is defined. Take element-1 as an example, the resistivity shown in [Figure 19 \(i\)](#) jumps to the upper limit of $10^{-8} \Omega \cdot \text{m}$ at load step-8, then calms down after load step-36 and finally “stabilizes” at $\sim 2.4 \times 10^{-11} \Omega \cdot \text{m}$; the resistivity shown in [Figure 19 \(j\)](#) jumps to $4.5 \times 10^{-10} \Omega \cdot \text{m}$ at load step-5, then calms down after load step-28 and finally “stabilizes” at $\sim 2.8 \times 10^{-12} \Omega \cdot \text{m}$; the resistivity shown in [Figure 19 \(k\)](#) jumps to $1.4 \times 10^{-14} \Omega \cdot \text{m}$ at load step-5, then calms down after load step-7 and finally “stabilizes” at $\sim 3.9 \times 10^{-14} \Omega \cdot \text{m}$.

5.3. Computation time and advantages

The above simulations are conducted on a HP-Z8-G4 workstation which uses Intel(R) Xeon(R) Gold 6128 CPU @ 3.40 GHz and 3.39 GHz (two processors, each one has 6 cores and 12 threads). For critical state model based FEA model, it is meshed with 11621 elements (35292 nodes) and takes 2~3 seconds to solve each load step; for flux creep model based FEA model, it is meshed with 11209 elements (40266 nodes) and takes 10~15 seconds to solve each load step. The flux creep model requires more time because it includes 6202 constraint equations which are used to couple \mathbf{A} between separated bulk elements.

Compared to COMSOL or other FEM tools, the advantages of using ANSYS-IAM for magnetization current simulation can be concluded as follows

a) The computation time for each load step of electromagnetic analysis is within several seconds or tens of seconds. The total computation time is adjustable because we can choose either to achieve

highly accurate simulation results (many iterative load steps) or to conduct the simulation case quickly (few iterative load steps).

b) The iterative-algorithm-method is based on ANSYS multi-frame restart analysis. Thus we can check the simulation results after any load steps and stop the program if we do not believe so-far result. Besides, it is feasible to restart the simulation from a solved load step. This is extremely beneficial when we have a more complicated FEA model in future which requires several days or weeks to solve one problem. In case of an accident of the workstation we can restart the simulation from where it stops.

c) The computation time can be saved when we use $\mathbf{A} \cdot \mathbf{V}$ formula in superconductor area and \mathbf{A} formula in non-superconductor area. This can be easily done in ANSYS by selecting proper degree of freedom.

d) There is no convergence difficulty when large n -value is specified in the flux creep model or ferromagnetic material exists in the whole FEA model. This iterative algorithm method is advantageous when the critical current density is highly non-linear and influenced by multiple factors (magnetic flux density, temperature, mechanical strain, magnetic field angle and etc.)

It is worth noting that the built-in form of Maxwell's equations in ANSYS can also be $\mathbf{Q} \cdot \mathbf{T} \cdot \mathbf{Q}$ formula through creating a new user-element [\[70\]](#). ANSYS is with “open-source” secondary development environment [\[71\]](#).

6. Conclusion

A series of magnetization simulations on disk-shaped ReBCO bulk are carried out by using ANSYS $\mathbf{A} \cdot \mathbf{V} \cdot \mathbf{A}$

formula based iterative algorithm method. This method is proved feasible to simulate the ReBCO bulk's magnetization current during ZFC or FC magnetization for both critical state model and flux creep model. It is also proved feasible to include ferromagnetic materials in the whole FEA model and to include J_c - B or J_c - ε dependence of the ReBCO bulk. Good solution accuracy can be achieved if we specify enough iterative load steps and select proper initial resistivity for the ReBCO bulk during magnetization simulation. Differing from the critical state model the specified magnetization time in the flux creep model can affect the simulation results significantly due to the relaxation of trapped current density in ReBCO bulk. Specially, there is a time-lag for the flux creep model based simulation results between using two different FEM tools. Compared to COMSOL or other FEM tools, ANSYS-IAM shows its unique advantages in manageable computation time, multi-frame restart analysis, easily used A - V - A formula and easy-convergence.

Acknowledgments

This work is supported by European Union's Horizon2020 research and innovation program under grant agreement No 777431.

References

- 1 Bottura L, Walckiers L and Wolf R 1997 *IEEE Trans. Appl. Supercond.* **7** 602-605
- 2 Green M A 1987 *IEEE Trans. Magn.* **23** 506-509
- 3 Hanft R W, Brown B C, Herrup D A, Lamm M J, McInturff A D and Syphers M J 1989 *IEEE Trans. Magn.* **25** 1647-1651
- 4 Bruck H, Gall D, Krzywinski J, Meinke R, Preißner H, Halemeyer M, Schmuser P, Stolzenburg C, Stiening R, Avest D and Klundert L J M 1991 *IEEE Partical Accelerator Conference* 2149-2151
- 5 Kashikhin V V and Zlobin A V 2001 *IEEE Trans. Appl. Supercond.* **11** 2058-2061
- 6 Karppinen M, Andreev N, Apollinari G, Auchmann B, Barzi E, Bossert R, Kashikhin V V, Nobrega A, Novitski I, Rossi L, Smekens D and Zlobin A V 2012 *IEEE Trans. Appl. Supercond.* **22** 4901504
- 7 Amemiya N, Sogabe Y, Sakashita M, Iwata Y, Noda K, Ogitsu T, Ishii Y and Kurusu T 2016 *Supercond. Sci. Technol.* **29** 024006
- 8 Amemiya N and Akachi K 2008 *Supercond. Sci. Technol.* **21** 095001
- 9 Yanagisawa Y, Kominato Y, Nakagome H, Hu R, Takematsu T, Takao T, Uglietti D, Kiyoshi T, Takahashi M and Maeda H 2011 *IEEE Trans. Appl. Supercond.* **21** 1640-1643
- 10 Yanagisawa Y, Nakagome H, Uglietti D, Kiyoshi T, Hu R, Takematsu T, Takao T, Takahashi M and Maeda H 2010 *IEEE Trans. Appl. Supercond.* **20** 744-747
- 11 Koyama Y, Takao T, Yanagisawa Y, Nakagome H, Hamada M, Kiyoshi T, Takahashi M and Maeda H 2009 *Physica C* **469** 694-701
- 12 Hahn S Y, Bascunan J, Kim W S, Bobrov E S, Lee H and Iwasa Y 2008 *IEEE Trans. Appl. Supercond.* **18** 856-859
- 13 Uglietti D, Yanagisawa Y, Maeda H and Kiyoshi T 2010 *Supercond. Sci. Technol.* **23** 115002
- 14 Ahn M C, Yagai T, Hahn S, Ando R, Bascunan J and Iwasa Y 2009 *IEEE Trans. Appl. Supercond.* **19** 2269-2272
- 15 Gu C, Qu T and Han Z 2007 *IEEE Trans. Appl. Supercond.* **17** 2394-2397
- 16 Yang D G, Kim K L, Choi Y H, Kwon O J, Park Y J and Lee H G 2013 *Supercond. Sci. Technol.* **26** 105025
- 17 Pardo E 2016 *Supercond. Sci. Technol.* **29** 085004
- 18 Kameari A 1990 *IEEE Trans. Magn.* **26** 466-469
- 19 Lousberg G P, Ausloos M, Geuzaine C, Dular P, Vanderbemden P and Vanderheyden B 2009 *Supercond. Sci. Technol.* **22** 055005
- 20 Stavrev S, Grilli F, Dutoit B, Nibbio N, Vinot E, Klutsch I, Meunier G, Tixador P, Yang Y and Martinez 2002 *IEEE Trans. Magn.* **38** 849-852
- 21 Fujishiro H and Naito T 2010 *Supercond. Sci. Technol.* **23** 105021

22 Fujishiro H, Naito T and Yoshida T 2014 *Supercond. Sci. Technol.* **27** 065019

23 Grilli F, Stravrev S, Floch Y L, Bouzo M C, Vinot E, Klutsch I, Meunier G, Tixador P and Dutoit B 2005 *IEEE Trans. Appl. Supercond.* **15** 17-25

24 Amemiya N, Murasawa S, Banno N and Miyamoto K 1998 *Physica C* **310** 16-29

25 Enomoto N and Amemiya N 2004 *Physica C* **412-414** 1050-1055

26 Stenvall A and Tarhasaari T 2010 *Supercond. Sci. Technol.* **23** 075010

27 Wang Y, Zhang M, Grilli F, Zhu Z and Yuan W 2019 *Supercond. Sci. Technol.* **32** 025003

28 Zhang H, Zhang M and Yuan W 2017 *Supercond. Sci. Technol.* **30** 024005

29 Liang F, Venuturumilli S, Zhang H, Zhang M, Kvitkovic J, Pamidi S, Wang Y and Yuan W 2017 *J. Appl. Phys.* **122** 043903

30 Kajikawa K, Hayashi T, Yoshida R, Iwakuma M and Funaki K 2003 *IEEE Trans. Appl. Supercond.* **13** 3630-3633

31 Hong Z, Campell A M and Coombs T A 2006 *Supercond. Sci. Technol.* **19** 1246-1252

32 Brambilla R, Grilli F and Martini L 2007 *Supercond. Sci. Technol.* **20** 16-24

33 Zhang M and Coombs T A 2012 *Supercond. Sci. Technol.* **25** 015009

34 Nguyen D, Ashworth S P, Willis J O, Sirois F and Grilli F 2010 *Supercond. Sci. Technol.* **23** 025001

35 Ainslie M D, Zermenio V M R, Hong Z, Yuan W, Flack T J and Coombs T A 2011 *Supercond. Sci. Technol.* **24** 045005

36 Tomita M and Murakami M 2003 *Nature* **421** 517-520

37 Durrell J H, Dennis A R, Jaroszynski J, Ainslie M D, Palmer K G B, Shi Y H, Campell A M, Hull J, Strasik M, Hellstrom E E and Cardwell D A 2014 *Supercond. Sci. Technol.* **27** 082001

38 Patel A, Baskys A, Williams T M, McCaul A, Coniglio W, Hanisch J, Lao M and Glowacki B A 2018 *Supercond. Sci. Technol.* **31** 09LT01

39 Ainslie M D, Fujishiro H, Mochizuki H, Takahashi K, Shi Y H, Namburi D K, Zou J, Dennis A R and Cardwell D A 2016 *Supercond. Sci. Technol.* **29** 074003

40 Hahn S, Kim S B, Ahn M C, Voccio J, Bascunan J and Iwasa Y 2010 *IEEE Trans. Appl. Supercond.* **20** 1037-1040

41 Zou S, Zermenio V M R, Baskys A, Patel A, Grilli F and Glowacki B A 2017 *Supercond. Sci. Technol.* **30** 014010

42 Yamamoto A, Ishihara A, Tomita M and Kishio K 2014 *Appl. Phys. Lett.* **105** 032601

43 Zhou D, Ainslie M D, Shi Y H, Dennis A R, Huang K, Hull J R, Cardwell D A and Durrell J H 2017 *Appl. Phys. Lett.* **110** 062601

44 Bean C P 1964 *Rev. Mod. Phys.* **36** 31-39

45 Pulmmer C J G and Evetts J E 1987 *IEEE Trans. Magn.* **23** 1179-1182

46 Rhyner J 1993 *Physica C* **212** 292-300

47 Ainslie M D and Fujishiro H 2015 *Supercond. Sci. Technol.* **28** 053002

48 Xu Z, Lewin R, Campell A M, Cardwell D A and Jones H 2012 *Supercond. Sci. Technol.* **25** 025016

49 Campbell A M 2009 *Supercond. Sci. Technol.* **22** 034005

50 Gu C and Han Z 2005 *IEEE Trans. Appl. Supercond.* **15** 2859-2862

51 Farinon S, Iannone G, Fabbricatore P and Gambrardella U 2014 *Supercond. Sci. Technol.* **27** 104005

52 Ainslie M D, Huang K Y, Fujishiro H, Chaddock J, Takahashi K, Namba S, Cardwell D A and Durrell J H 2019 *Supercond. Sci. Technol.* **32** 034002

53 Gu C, Qu T, Li X and Han Z *IEEE Trans. Appl. Supercond.* **23** 8201708

54 Ainslie M and Zou J 2015 Benchmark test HTS modelling http://www.htsmodelling.com/?wpdmpro=b4_results

55 Fujishiro H, Kaneyama M, Tateiwa T and Oka T 2005 *Jpn. J. Appl. Phys.* **44** 1221-1224

56 Kim Y B, Hempstead C F and Strand A R 1962 *Phys. Rev. Lett.* **9** 306-309

57 Anderson P W 1962 *Phys. Rev. Lett.* **9** 309-311

58 Barth C, Mondonico and Senatore C 2015 *Supercond. Sci. Technol.* **28** 045011

59 Laan D C, Weiss J D, Noyes P, Trociewitz U P, Godeke A, Abraimov D and Larbalastier D C 2016 *Supercond. Sci. Technol.* **29** 055009

60 Cheggour N, Ekin J W, Thieme C L H, Xie Y Y, Selvamanickam V and Feenstra R 2005 *Supercond. Sci. Technol.* **18** 319-324

61 Takayasu M, Chiesa L, Bromberg L and Minervini J V 2012 *Supercond. Sci. Technol.* **25** 014011

62 Godeke A, Hartman M H C, Mentink M G T, Jiang J, Matras M, Hellstrom E E and Larbalestier D C 2015 *Supercond. Sci. Technol.* **28** 032001

63 Larbalestier D C, Jiang J, Trociewitz U P, Kametani F, Scheuerlein C, Canassy M D, Matras M, Chen P, Craig N C, Lee P J and Hellstrom E E 2014 *Nature Mat.* **13** 375-381

64 Zhang K, Higley H, Ye L, Gourlay S, Prestemon S, Shen T, Bosque E, English C, Jiang J, Kim Y, Lu J, Trociewitz U P, Hellstrom E E and Larbalestier D C 2018 *Supercond. Sci. Technol.* **31** 105009

65 Trociewitz U P, Canassy M D, Hannion M, Hilton D K, Jaroszynski J, Noyes P, Viouchkov Y, Weijers H W and Larbalestier D C 2011 *Appl. Phys. Lett.* **99** 202506

66 Iwasa Y, Bascunan J, Hahn S, Voccio J, Kim Y, Lecrevisse T, Song J and Kajikawa K 2015 *IEEE Trans. Appl. Supercond.* **25** 4301205

67 Matsumoto S, Kiyoshi T, Otsuka A, Hamada M, Maeda H, Yanagisawa Y, Nakagome H and Suematsu H 2012 *Supercond. Sci. Technol.* **25** 025017

68 Wang Q, Liu J, Song S, Zhu G, Li Y, Hu X and Yan L 2015 *IEEE Trans. Appl. Supercond.* **25** 4603505

69 Hahn S, Kim K, Kim K, Hu X, Painter T, Dixon I, Kim S, Bhattacharjee K R, Noguchi S, Jaroszynski J and Larbalestier D C 2019 *Nature* **570** 496-499

70 Testoni P 2003 Implementation in the ANSYS finite element code of the electric vector potential $T\mathcal{Q}$, \mathcal{Q} formulation and its validation with the magnetic vector potential $A\mathcal{V}$, A formulation *PhD Thesis* University of cagliari
http://www.diee.unica.it/DRIEI/tesi/15_testoni.pdf

71 Brouwer L, Arbelaze D, Auchmann B, Bortot L and Stubberud E 2019 *Supercond. Sci. Technol.*
<https://doi.org/10.1088/1361-6668/ab2e63>